

Anodic oxide films of nickel in alkaline electrolyte

Visscher, W.H.M.; Barendrecht, E.

Published in:
Surface Science

DOI:
[10.1016/0039-6028\(83\)90235-2](https://doi.org/10.1016/0039-6028(83)90235-2)

Published: 01/01/1983

Document Version
Publisher's PDF, also known as Version of Record (includes final page, issue and volume numbers)

Please check the document version of this publication:

- A submitted manuscript is the author's version of the article upon submission and before peer-review. There can be important differences between the submitted version and the official published version of record. People interested in the research are advised to contact the author for the final version of the publication, or visit the DOI to the publisher's website.
- The final author version and the galley proof are versions of the publication after peer review.
- The final published version features the final layout of the paper including the volume, issue and page numbers.

[Link to publication](#)

General rights

Copyright and moral rights for the publications made accessible in the public portal are retained by the authors and/or other copyright owners and it is a condition of accessing publications that users recognise and abide by the legal requirements associated with these rights.

- Users may download and print one copy of any publication from the public portal for the purpose of private study or research.
- You may not further distribute the material or use it for any profit-making activity or commercial gain
- You may freely distribute the URL identifying the publication in the public portal ?

Take down policy

If you believe that this document breaches copyright please contact us providing details, and we will remove access to the work immediately and investigate your claim.

ANODIC OXIDE FILMS OF NICKEL IN ALKALINE ELECTROLYTE

W. VISSCHER and E. BARENDRECHT

Laboratory of Electrochemistry, Eindhoven University of Technology, P.O. Box 513, 5600 MB Eindhoven, The Netherlands

Received 28 January 1983; accepted for publication 2 June 1983

Cyclic voltammetry and ellipsometry were applied to investigate the growth and nature of the anodic oxide film on nickel in 0.1M KOH. At prerduced nickel a poorly conducting oxide is formed which grows with constant refractive index in the potential range up to about 1 V. At higher potentials the changes in the ellipsometric parameters ψ and Δ indicate a conversion into a good conducting oxide. By repeated oxidation and reduction a thicker oxide film is grown at the surface, this oxide is not identical with the anodically grown films as is shown by its different refractive index. From comparison with data for α - and β -Ni(OH)₂ it is concluded that the film formed at anodic potentials up to about 1 V must be considered to be NiO·xH₂O.

1. Introduction

The anodic behaviour of nickel is of interest because of the many applications of nickel. The use of nickel in alkaline batteries has oriented the research towards oxidation and reduction of thick nickel hydroxide-film electrodes prepared by deposition of Ni(OH)₂ onto a substrate. The application of nickel as anode in many electrolyses has focussed the study on the oxidation of nickel and the formation of passive films. Cyclic voltammetry and ellipsometry have proved to be useful techniques in revealing surface processes. The reduction of surface oxides is difficult; the electrochemical behaviour of nickel depends upon its previous history resulting in different voltammograms depending on the pretreatment [1-3], as shown in fig. 1.

About the nature and the thickness of the anodic oxide layer different opinions are given. The passive film is found to be potential dependent in borate buffer [4], in sulphate [5], phosphate [6] and alkaline [7,8] electrolytes, while a constant thickness is observed by MacDougall and Cohen [9] in neutral (pH = 8.4) solutions. In borate buffer the nature of the film is most likely to be NiO [4,10], whereas Okuyama and Haruyama [11] conclude to a duplex or mixed layer consisting of NiO and Ni₃O₄. Ord et al. [5] assume that NiO is formed during the first anodic cycle and thereafter is converted to Ni(OH)₂ during vigorous reduction, while Chao and Szklarska-Smialowska [6] conclude

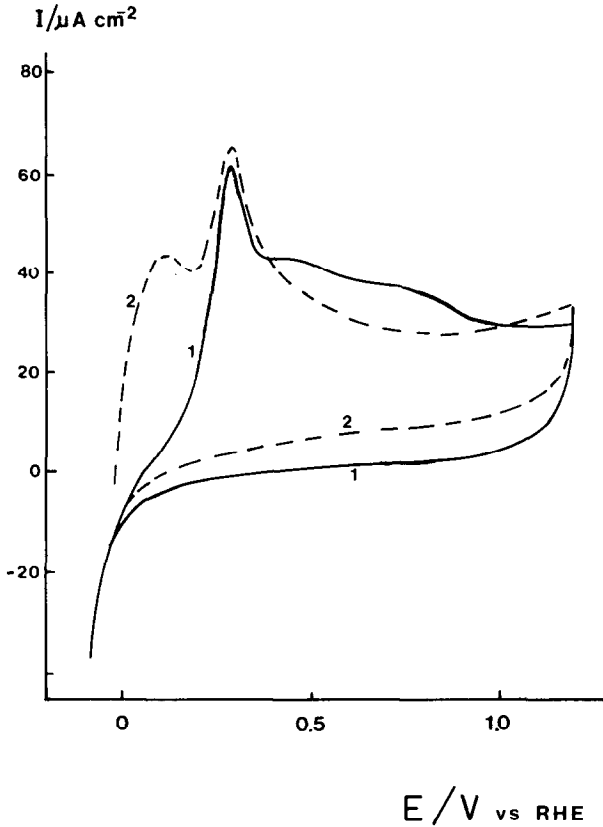


Fig. 1. Voltammogram of Ni in alkaline electrolyte; scan rate 10 mV s^{-1} . Pretreatment: (1) polishing and cathodic reduction; (2) polishing, cathodic reduction and thereafter repeated potential cycling from -0.8 to $+1.2 \text{ V}$ versus RHE [3].

to initial formation of $\text{Ni}(\text{OH})_2$ (in phosphate buffer) which thereafter partially dehydrates.

In alkaline solution, Paik and Szklarska-Smialowska [7] find that the refractive index of the oxide layer changes continuously and explain this as gradual dehydration of $\text{Ni}(\text{OH})_2$ to NiO . On the basis of the refractive indices of film $\text{Ni}(\text{OH})_2$ electrodes, Hopper and Ord [12] assume that the reduced form of oxidized nickel is $\beta\text{-Ni}(\text{OH})_2$. The oxidation to higher valency oxides proceeds either gradually [2] with "conjugate redox couples" [3,13] or via different stages from NiO to Ni_3O_4 and to Ni_2O_3 [10,11,14,15].

The objective of this paper is to examine the first anodic oxide film on Ni in alkaline solutions by ellipsometry and cyclic voltammetry and to compare the results with data obtained at $\text{Ni}(\text{OH})_2$ film electrodes.

2. Experimental

The optical cell was a KelF cylindrical vessel with quartz windows fixed for angle of incidence of 70° at the mounted working electrode. The cell contains a Pt counter electrode, gas inlet tubing and a Luggin capillary placed close to the working electrodes and connected to the Pt hydrogen reference electrode compartment. All potentials are referred to this reference electrode. For cyclic-voltammetric studies a three-compartment cell was used, also with a Pt counter electrode and a Pt hydrogen reference electrode.

The Ni electrode consisted of a nickel disc (99.99%), mounted in a perspex or KelF holder with exposure of one side to the electrolyte. Before each experiment the nickel electrodes was pretreated to either a "prereduced" or a "precycled" state.

Procedure for "prereduced" electrode: Nickel was carefully polished with alumina down to finally $0.3 \mu\text{m}$, then reduced in $1\text{M H}_2\text{SO}_4$ under vigorous H_2 evolution, rinsed with distilled H_2O and immediately thereafter transferred to the cell. In the cell the potential was first held at $E = -1000 \text{ mV}$ versus RHE and then set at $E = -100 \text{ mV}$. The ellipsometric readings taken at this potential were considered to represent the bare substrate since the values did not change with repeated reduction at -1000 mV .

Procedure for "precycled" electrode: Firstly a "prereduced" electrode is prepared, this is thereafter subjected to repeated anodic and cathodic potential cycles from -800 and $+1200 \text{ mV}$ in 0.1M KOH . This treatment has been found [3] to yield a reproducible voltammogram. The optical measurements were conducted with a Rudolph automatic ellipsometer, model RR 2000, equipped with a tungsten iodine light source and a monochromatic filter for 5461 \AA . In some experiments a 5000 or 6500 \AA filter was applied.

Potential sweep measurements were performed with a PAR model 175 Universal Programmer with a Wenking potentiostat. The electrolyte was 0.1M KOH prepared from p.a. grade and double distilled water.

3. Results

3.1. Oxidation of prereduced nickel

The optical behaviour of nickel during an applied anodic potential scan from -100 to $+1500 \text{ mV}$ at 0.5 mV/s is shown in fig. 2. With increasing anodic potential Δ decreases, while ψ first increases and beyond 1300 mV begins to decrease. During the cathodic scan Δ and ψ go back to the values reached at ca. 1300 mV during the anodic scan and do not return to the original values. This result is typical for potential scans with $1400 \leq E_{\text{return}} \leq$

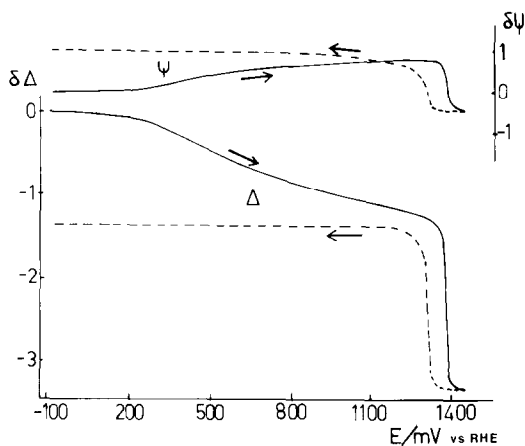


Fig. 2. Ellipsometric response to potential cycle -0.1 to $+1.5$ V applied to prereduced Ni-electrode in 0.1M KOH ; scan rate 0.5 mV s^{-1} . Changes in Δ and ψ are given with respect to their values at $E = -0.1$ V.

1650 mV. For lower E_{return} potentials ($900 \leq E_{\text{return}} \leq 1400$ mV), Δ and ψ remain constant during the whole reverse sweep as is shown in fig. 3 for $E_{\text{return}} = 1200$ mV. Fig. 4 gives the corresponding voltammogram. Stepwise increase of the potential from $E = -100$ to 1500 mV and back (with 1 min hold of the potential at each step) gives a similar pattern for Δ and ψ (fig. 5). The results of fig. 5 are replotted in fig. 6 in a ψ - Δ graph. The initial rise in ψ is

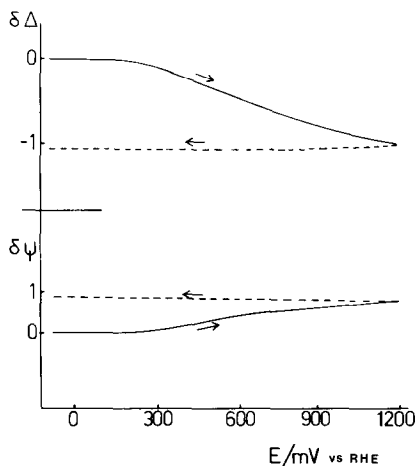


Fig. 3. Change in Δ and ψ during cycling of prereduced Ni-electrode in 0.1M KOH from -0.1 to $+1.2$ V; scan rate 0.5 mV s^{-1} .

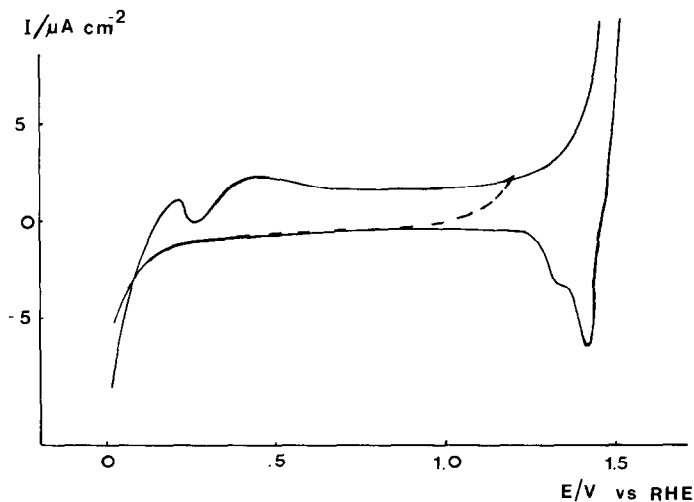


Fig. 4. Voltammogram of prerduced Ni in 0.1M KOH; scan rate 0.5 mV s^{-1} ; scan -0.1 to $+1.5$ V (—), and -0.1 to $+1.2$ V (---).

only observed if a freshly polished nickel electrode has been given the pretreatment involving cathodic reduction in $1\text{M H}_2\text{SO}_4$ to remove any existing surface oxides.

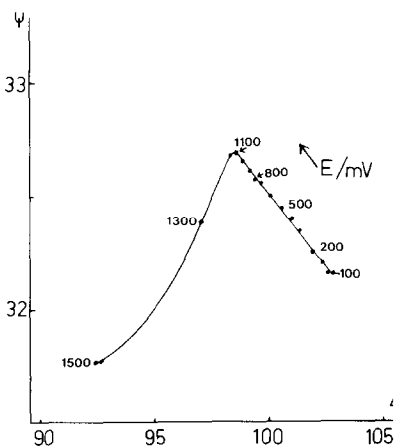
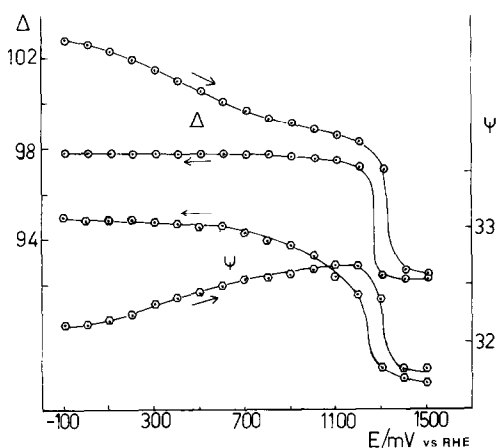


Fig. 5. ψ and Δ at prerduced Ni-electrode in 0.1M KOH for stepwise increasing and decreasing potential with 1 min hold of the potential at each step.

Fig. 6. Graph of ψ versus Δ for results of fig. 4, numbers along the curve refer to potential values.

Table 1
Ni oxidation at 500 mV versus RHE for 1 h

Ellipsometry			Coulometry (mC/cm ²)
$\delta\Delta$	$\delta\psi$	Wavelength (Å)	
-3.04	+0.56	5000	1495
-2.90	+0.46	5461	
-2.59	+0.40	6500	

$$\delta\Delta = \Delta_{\text{final}} - \Delta_{\text{initial}}; \delta\psi = \psi_{\text{final}} - \psi_{\text{initial}}$$

The oxide formed in the lower potential region was further investigated by applying for 1 h a constant potential of 500 mV to a prerduced electrode. In this series of experiments both coulometric and optical changes were measured. The optical data were taken at 5000, 5461 and 6500 Å. The results are given in table 1.

3.2. Oxidation of precycled nickel

The optical response of a "precycled" nickel electrode to an anodic potential scan shows a much smaller effect in the lower potential region. Fig. 7 gives the Δ and ψ change for a -100 to 1200 mV scan at 10 mV/s and also the corresponding voltammogram. The change in ψ with increasing potential sets in at a lower potential than at a prerduced electrode, with a shallow maximum at 700–800 mV.

The reduction behaviour of a precycled electrode depends upon the applied potential scan: for potential sweeps with $E_{\text{return}} < 900$ mV the oxide formed during that cycle is reduced as is indicated by the cathodic peak at 0 V and is also evident from the final Δ and ψ values. Fig. 8 gives the ellipsometric Δ and voltammetric results for $E_{\text{return}} = 500$ mV. Fig. 9 compares Δ - E plots for $E_{\text{return}} = 300, 500, 700$ and 900 mV (since the change in ψ is very small, the ψ - E plots are omitted) and fig. 10 gives the corresponding I - E plots. Between each of these cycles the electrode was given an oxidation-reduction cycle from -800 to +1200 mV and then hold at -300 mV before the next run was started. Fig. 9 shows that after a potential scan to $E_{\text{return}} < 700$ mV, Δ returns to its value at the beginning of that cycle within 0.06°; for $700 < E_{\text{return}} < 900$ mV, a cathodic reduction at -300 mV was required to bring Δ back to the original value. If $E_{\text{return}} > 900$ mV, Δ does not return to its begin value.

The voltammogram of precycled nickel in the potential region 1.0–1.6 V shows an anodic peak at 1440 mV and a cathodic peak at 1380 mV with a shoulder at 1300 mV (fig. 11). If the reduction cycle is extended to -800 mV before the next anodic sweep, then a double anodic peak becomes manifest at respectively 1380 (peak A) and 1440 mV (peak B), fig. 12. With continued

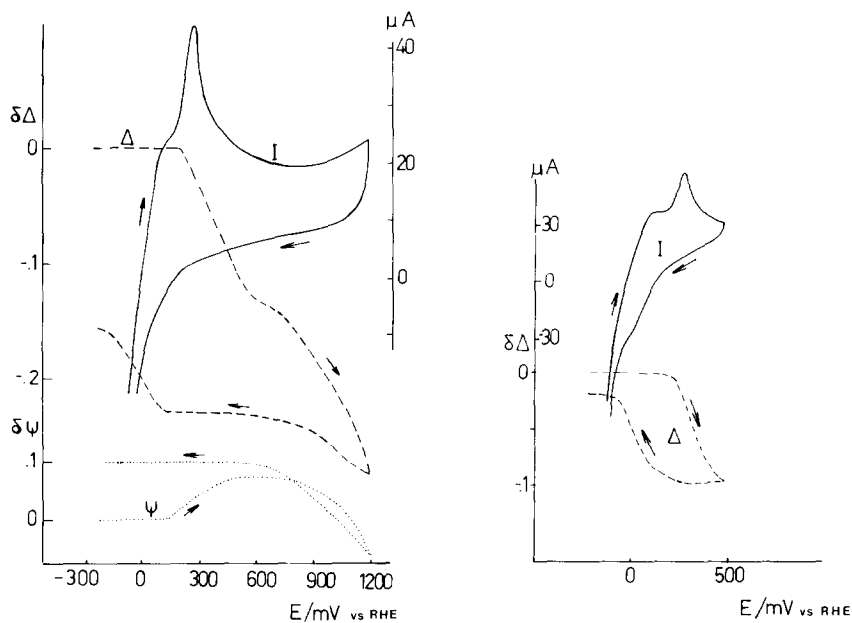


Fig. 7. Cyclic voltammogram and ellipsometric curves for "precycled" Ni-electrode; potential scan -0.1 to 1.2 V; scan rate 10 mV s^{-1} ; electrode area 0.7 cm^2 .

Fig. 8. Voltammogram and $\Delta-E$ curve at precycled Ni-electrode with $E_{\text{return}} = 500 \text{ mV}$; scan rate 10 mV s^{-1} ; electrode area 0.7 cm^2 .

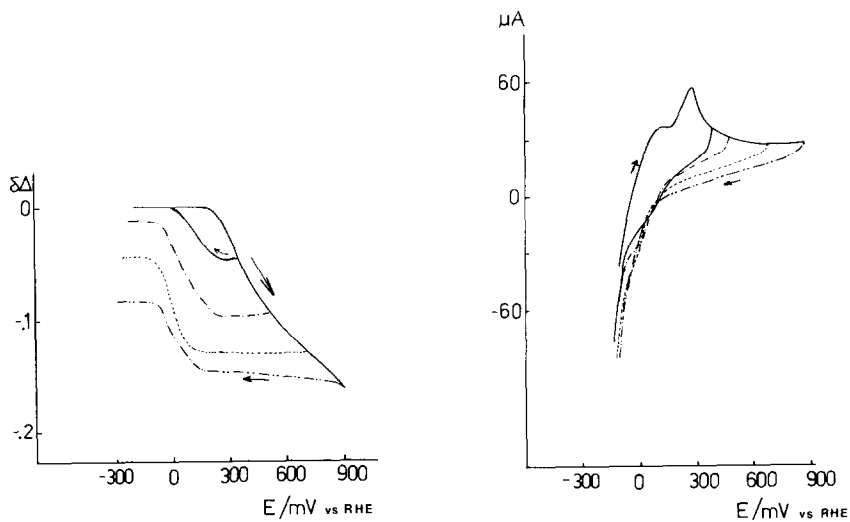


Fig. 9. $\Delta-E$ curves at precycled Ni-electrode with $E_{\text{return}} = 300 \text{ mV}$ (---), 500 mV (-·-·-·-·), 700 mV (·····) and 900 mV (- - - - -); scan rate 10 mV s^{-1} .

Fig. 10. Voltammograms corresponding with the optical data of fig. 9; electrode area 0.7 cm^2 .

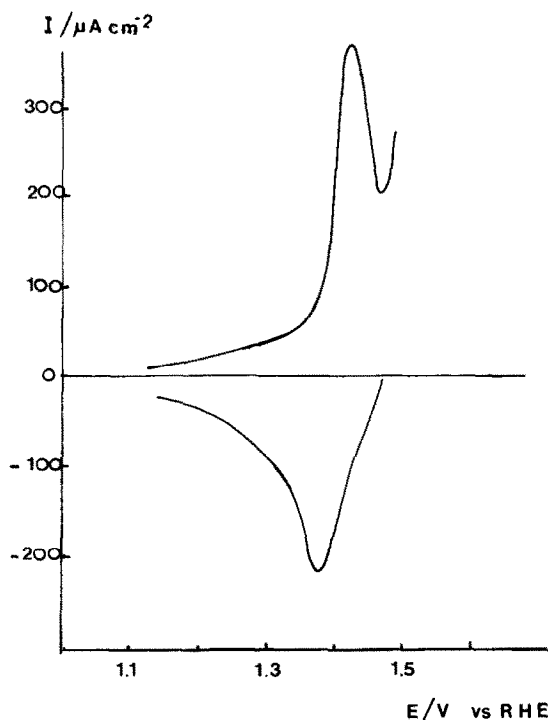


Fig. 11. Voltammogram of precycled Ni-electrode in potential range $1.0 \leq E \leq 1.6$ V; scan rate 10 mV s^{-1} .

cycling the peaks shift in anodic direction and finally disappear in the O_2 evolution current (cycle 24 in fig. 12). When a potential scan is applied with E_{return} between E_A and E_B , the voltammogram shows only the most cathodic peak indicating that peak a is related to peak A and peak b to B. For comparison the voltammogram of prerduced Ni is given in fig. 13.

4. Discussion

4.1. Nickel oxidation at $0 < E < 1$ V

The refractive index of prerduced nickel as calculated from Δ and ψ values at $E = -100$ mV in 0.1M KOH is given in table 2. These results are in good agreement with literature data for nickel as compiled in table 3.

The oxidation of Ni starts at 0–200 mV depending on the oxidation mode as is shown by the optical results of figs. 2, 3 and 5. With increasing anodic

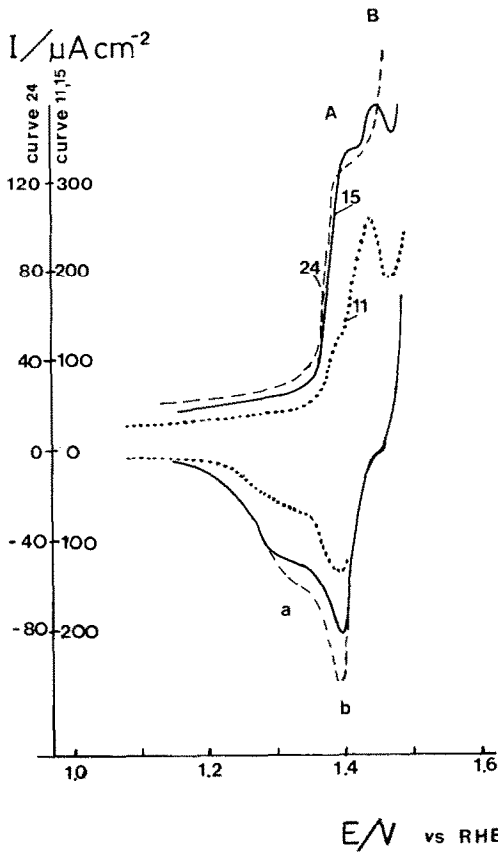


Fig. 12. Voltammogram of precycled Ni-electrode with reduction sweep to -0.8 V before the next anodic sweep is applied; 11th, 15th and 24th cycle; scan rate 10 mV s^{-1} .

potential the change of Δ and ψ is such that a linear ψ - Δ relation is obtained in the lower potential region.

This implies that, up to about 1 V, an oxide is formed which grows with *constant* refractive index. In some runs the ψ - Δ plot shows a slight deviation

Table 2
Refractive index ($n - ik$) of Ni in 0.1M KOH

n	k	Wavelength (\AA)
1.753	3.289	5000
1.887	3.449	5461
2.340	4.001	6500

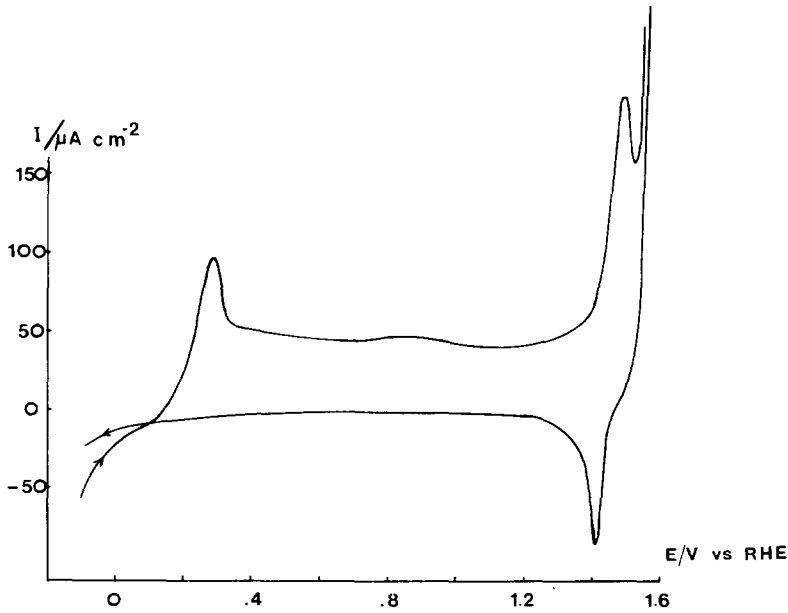


Fig. 13. Voltammogram of prerduced Ni; scan rate 10 mV s^{-1} .

Table 3
Literature data of the refractive index ($n - ik$) of nickel

Wavelength (\AA)	n	k	Medium	Ref.
5000	1.54	2.975		[16]
	1.73	3.12	H_2SO_4	[18]
5461	1.59	3.27		[16]
	1.793	3.281	$\text{H}_2\text{SO}_4 - \text{K}_2\text{SO}_4$	[19]
	1.79	3.29		[20]
	1.65	3.81	Borate buffer	[4]
	1.75-1.83	3.24-3.57	Air	[21]
	1.52	2.64	KOH	[22]
	1.73	3.47	NaOH	[7]
	1.68	3.63	Phosphate buffer	[6]
5890	2.47	3.05	KOH	[23]
	1.87	3.36	KOH	[3]
5890	1.79	3.33		[24]
6328	2.13	4.31	KOH	[12]
	2.147	4.239	Na_2SO_4	[5]
	2.04	3.43	KOH	[25]
6500	1.91	3.93		[16]

from 700 mV on. The change in ψ at $E > 1$ V coincides with the onset of a further oxidation process. The ψ maximum is not observed at a definite potential but rather over a potential region; with lower scan rates $E_{\psi_{\max}}$ is also lower.

The properties of the oxide formed at 500 mV were calculated for the data of table 1. The coulometric value indicates that after 1 h a film of 3 to 4 monolayers has been formed. For conversion into thickness, knowledge of the specific oxide type is required. It is not unambiguously known, however, what kind of nickel oxide is formed during anodic oxidation. Usually, it is assumed that in alkaline solutions nickel hydroxide is formed, but it has not yet been established whether this hydroxide is identical with, e.g., α -Ni(OH)₂ (3Ni(OH)₂ · 2H₂O), which is formed by cathodic deposition from a Ni(NO₃)₂ electrolyte or with β -Ni(OH)₂, which is obtained by conversion of α -Ni(OH)₂ [31]. With specific mass data for these species [31], the thickness (d) is calculated. This gives $d = 31.1$ Å for α -Ni(OH)₂, with $\rho = 2.62$ g/cm³, $d = 18.5$ Å for β -Ni(OH)₂ with $\rho = 3.9$ g/cm³ and $d = 8.5$ Å for NiO with $\rho = 6.8$ g/cm³. From the ellipsometric data thickness and refractive index were obtained using the McCrackin program [27].

Within the range $1.4 \leq n \leq 3$ and $0 \leq k \leq 1$, solutions were sought for the film, yielding a series of d , n , k values. The results are summarized in fig. 14 for six experiments at 5461 Å. The lowest d values are obtained if $k = 0$. Averaging the data with $k = 0$ gives:

$$d = 17.0 \text{ \AA}, \quad n = 2.27, \quad \text{at } \lambda = 5461 \text{ \AA},$$

$$d = 19.5 \text{ \AA}, \quad n = 1.98, \quad \text{at } \lambda = 5000 \text{ \AA},$$

$$d = 18.5 \text{ \AA}, \quad n = 1.95, \quad \text{at } \lambda = 6500 \text{ \AA}.$$

These values appear to be in close agreement with the coulometric thickness values calculated for β -Ni(OH)₂ for which conversion no roughness factor was introduced.

Since no lower d values are found, no agreement can be obtained if the layer was supposed to be NiO. If the layer is assumed to be α -Ni(OH)₂, then the optical data for $d = 31.1$ Å are sorted out. This results in

$$n = 1.69 - 0.052i, \quad \text{at } \lambda = 5461 \text{ \AA},$$

$$n = 1.68 - 0.020i, \quad \text{at } \lambda = 5000 \text{ \AA},$$

$$n = 1.69 - 0.020i, \quad \text{at } \lambda = 6500 \text{ \AA}.$$

There appears to be no appreciable change in n with wavelength; the low k value is to be expected for a poorly conducting film.

On the basis of these results it cannot yet be concluded which species is formed by anodic oxidation.

Different values are quoted in the literature for nickel(II) oxides, as can be seen from table 4. It must be remarked that some of these results were obtained with certain assumptions about the oxide layer.

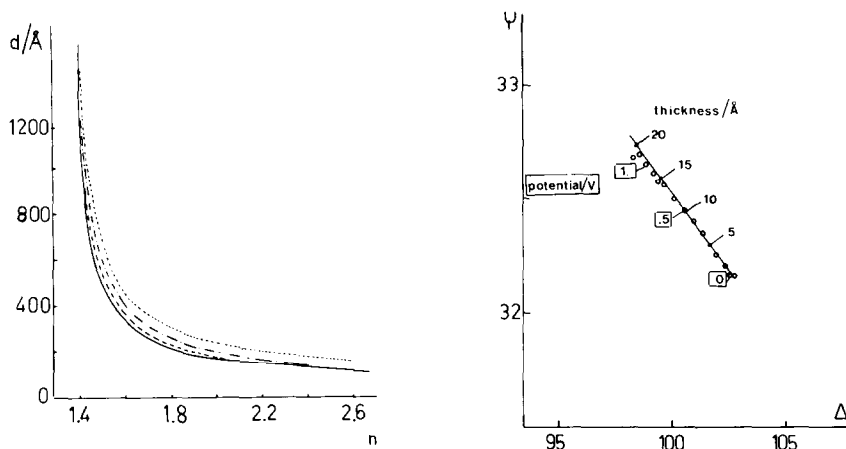


Fig.14. Series of solutions of refractive index (n) and thickness (d) for anodic oxide film at $E = 0.5$ V, grown for 1 h at pre-reduced Ni; $\lambda = 5461$ Å.

Fig. 15. Thickness of anodic oxide with refractive index $n - ik = 2.45 - 0i$ in potential range $E = 0$ to 1.1 V.

Our results agree with data of others (cf. table 4) for oxidation in alkaline media, though Paik and Szklarska-Smialowska [7] conclude to a continuously changing refractive index for the oxide up to 1.38 V. A constant value for the refractive index in the lower potential region, as observed here, is also in agreement with voltammetric results which show no appreciable change in the anodic current up to 0.9 V as would be expected if k varies. Similarly, galvanostatic experiments of Damjanovic et al. [32] show a linear rise of potential with time up to ca. 1.3 V indicating field assisted formation of the oxide layer. The results show that the oxide layer grows with increasing anodic potential. For the data of the potential step experiments (fig. 5) the best fit was obtained with $n = 2.45 - 0i$. This is represented in fig. 15; it can be concluded that in this experiment the film grows to about 20 Å at 1100 mV, whereafter a further oxidation begins.

At the maximum in the ψ - Δ curve, the optical properties change. This change occurs over a potential range and is affected by the pretreatment of the electrode and the oxidation mode. A maximum was also observed by others [6,25,28,29], but not at the same potentials. The present results show a maximum with potentiostatic oxidation at 1.2 V at a pre-reduced electrode and a shallow maximum at 0.6 V at a precycled electrode.

The oxidation of Ni(II) oxide to NiOOH takes place via H^+ transport through the oxide film [12]. Since this film is a poor conductor, the oxidation

Table 4
Refractive index ($n - ik$) for divalent nickel oxide and hydroxide species

Species	Medium	Wavelength (Å)	n	k	Ref.
NiO		5500	2.23		[17]
NiO		6710	2.37		[17]
NiO	Air	5461			[21]
	a)		2.9	0.09	
	b)		2.6	0.16	
	c)		3.0	0.2	
NiO	14N H ₂ SO ₄	5000	1.5–1.7	0.06–0.1	[27]
NiO	1N H ₂ SO ₄	5000	2.10	0.46	[18]
NiO	0.15 N Na ₂ SO ₄	6328	1.775	0.234	[5]
NiO/Ni(OH) ₂	Phosphate buffer	5461	2.2	0.11	[6]
NiO	Borate buffer	5461	2.7	0.25	[4]
Ni(OH) ₂	KOH	6328	2.8	0.1	[8]
Ni(OH) ₂	KOH	5461	1.55	0	[28]
Ni(OH) ₂	KOH	5461	2.6	0–0.2	[29]
Ni(OH) ₂ ^{d)}	KOH	5461	1.45–1.55	0–0.03	[3]
Ni(OH) ₂ /NiO	NaOH	5461	2.0–2.5	0.05	[7]
α -Ni(OH) ₂ ^{e)}	Ni(NO ₃) ₂	5461	1.41	0	[35]
α -Ni(OH) ₂ ^{e)}	Ni(NO ₃) ₂	6328	1.52	0	[12]
α -Ni(OH) ₂ ^{e)}	Ni(NO ₃) ₂	6328	1.502	0	[30]
β -Ni(OH) ₂ ^{f)}	KOH	6328	1.46	0	[12]
β -Ni(OH) ₂ ^{g)}	Ni(NO ₃) ₂	6328	1.43	0	[30]
β -Ni(OH) ₂ ^{h)}	Ni(NO ₃) ₂	5461	1.46	0	[35]

a) Air oxidation 100–200°C.

b) Air oxidation 250–300°C.

c) Air oxidation 300–400°C.

d) Film grown by repeated anodization at 0.4 V followed by reduction.

e) Cathodically deposited.

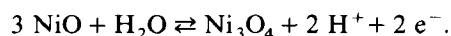
f) "Reduced oxide": formed by anodic and cathodic cycling of nickel; assumed to be β -Ni(OH)₂.

g) Species produced by oxidation and reduction of α -Ni(OH)₂; assumed to be β -Ni(OH)₂.

h) Obtained by conversion of α film.

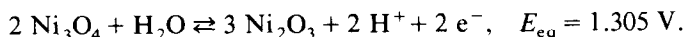
process must start at the metal–oxide interface with the protons moving to the oxide–electrolyte interface.

It seems likely that the Ni(II)–Ni(III) conversion proceeds in parallel with the direct oxidation of Ni to Ni(II) that continues at these potentials. Now the conversion of Ni(II) to Ni(III) species is observed as a peak in the cyclic voltammograms at about 1.3–1.4 V whereas the optical data indicate already a change in film properties, at lower potentials. The oxidation starts at $E \geq 0.876$ V being the equilibrium potential [33] for



As soon as the composition of the film is equivalent to Ni₃O₄, the oxidation

proceeds [33] to NiOOH



This process is characterized by a current peak in the voltammogram. The oxidation to Ni_3O_4 proceeds gradually and is not manifest in the voltammogram. Optically, this conversion can be considered as a two-film system with 2 different refractive indices. This explains the rather broad maximum of the ψ - Δ curves.

4.2. Precycled electrode

It has been reported that cycling changes the properties of the nickel surface. This is characterized by the two anodic peaks in the voltammogram in the potential range 0–500 mV (e.g. fig. 8). The peak at ca. 70 mV has been attributed to absorbed hydrogen [34]. This peak is *not* observed in the ellipsometric scan, so H_{abs} either does not affect the optical density or does not represent a real phase. The nickel oxide formed during anodic oxidation is only partially reduced during cathodic cycling, as is clearly demonstrated by comparing the Δ and ψ values at $E = -300$ mV after repeated cycling. Fig. 16 shows that with cycling Δ decreases and ψ increases, indicating the growth of a film.

The conversion of this film to a higher valency oxide begins at a less anodic potential, probably due to the more loose structure of the oxide. The reduction diagrams (figs. 7 to 10) demonstrate that complete reduction of the anodically formed oxide is only realized if the anodic potential does not exceed ca. 900

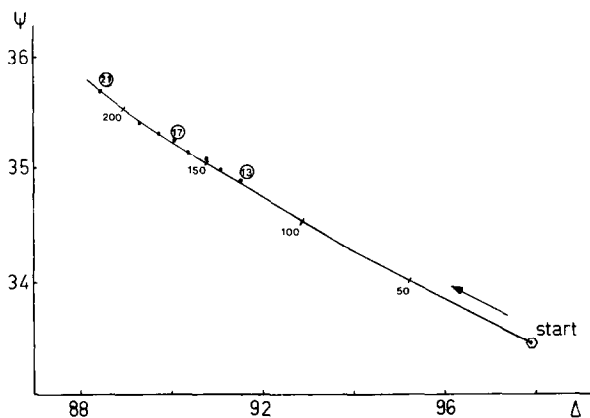


Fig. 16. Growth of oxide film by repeated cycling; (●) experimental ψ , Δ data; numbers in circles indicate cycle number. The drawn line gives the calculated Δ - ψ plot for $n - ik = 1.52 - 0i$ for increasing thickness values in Å.

mV, so the reduced form of the trivalent (or higher) oxide cannot be identical to the anodically formed divalent oxide. This is supported by the optical data of fig. 16. Evaluation, assuming a substrate–film–electrolyte system, yields a refractive index $n - ik = 1.52 - 0i$ for the film. This refractive index value agrees with data of Hopper and Ord [12] for reduced oxide film and is also in accordance with the value for a film grown on Ni by repeated oxidation at 0.4 V followed by reduction [3]. In fig. 16 the increase of thickness with cycling is indicated, after 20 cycles a value of 200 Å is reached.

4.3. Which nickel(II) oxide species is formed?

The n -value obtained for the oxide film at the precycled electrode differs substantially from the n -value for the oxide film at the prerduced electrode. It is thus clear these films cannot be the same oxide layer. The refractive index of the reduced oxide lies in the same range as the n values for α - and β -Ni(OH)₂ (cf. table 4).

The electrochemical behaviour of nickel and of Ni(OH)₂ films shows a close resemblance in the potential region 1–1.6 V. At Ni(OH)₂ film electrodes, prepared by cathodic deposition, we observed, as published elsewhere [35] characteristic peak potentials for α -Ni(OH)₂ and for β -Ni(OH)₂. In table 5 these peak potentials are summarized together with those for Ni at a scan rate of 10 mV s⁻¹. The coincidence of the anodic peak of Ni with that of β -Ni(OH)₂ could suggest that the anodic film is β -Ni(OH)₂; however in the reduction scan of Ni a double peak is observed which seems to imply that during the reduction two species are formed: α - and β -Ni(OH)₂. With vigorous reduction between oxidation cycles, cf. fig. 12, this α -type becomes apparent in the anodic sweep as well.

From the n data of the layer grown at 500 mV at the prerduced electrode, it is concluded that this layer cannot be a Ni(OH)₂ species, notwithstanding the fact that its optical thickness agrees with the coulometric thickness when the bulk density of β -Ni(OH)₂ is used in the conversion factor. Another possibility is that the layer is a NiO species. It is noted that for air-oxidized

Table 5

Anodic and cathodic peak potentials in cyclic voltammogram for $E > 1$ V

	E_p^{anodic} (V)	E_p^{cathodic} (V)
α -Ni(OH) ₂	1.385	1.295
β -Ni(OH) ₂	1.455	1.27
Ni prerduced	1.48	1.41
Ni precycled	1.44	1.38
Ni with reduction between cycles	1.38, 1.44	1.30, 1.38

nickel n values between 2 and 3 have been found. NiO is usually suggested as the first oxide in acid or neutral solution. If the anodic film in alkaline solution consists of NiO, then a lower density value is required in order to bring agreement between the coulometric and ellipsometric data. A value of $\rho = 3.13 \text{ g/cm}^3$ for the specific mass would satisfy. Such a decrease in ρ can be attributed to water uptake (ca. 40%) by the film.

It is a matter of debate, of course, whether indeed a thin hydroxide layer has identical properties as the bulk oxide. In conclusion, the results of this work show that during anodic oxidation of Ni initially a thin passive layer of $\text{NiO} \cdot x\text{H}_2\text{O}$ is formed which grows with increasing anodic potential till ca. 1 V up to a few monolayers. Electrochemically the film behaves as $\beta\text{-Ni(OH)}_2$. With repeated oxidation and reduction the composition of this layer changes to Ni(OH)_2 and its thickness increases.

References

- [1] J.C. Weininger and M.W. Breiter, *J. Electrochem. Soc.* 111 (1964) 707.
- [2] R.S. Schrebler Guzman, J.R. Vilche and A.J. Arvia, *Electrochim. Acta* 8 (1978) 67.
- [3] W. Visscher and E. Barendrecht, *Electrochim. Acta* 25 (1980) 651.
- [4] N. Sato and H. Kudo, *Electrochim. Acta* 19 (1974) 461.
- [5] J.L. Ord, J.C. Clayton and D.J. DeSmet, *J. Electrochem. Soc.* 124 (1977) 1714.
- [6] C.Y. Chao and Z. Szklarska-Smialowska, *Surface Sci.* 96 (1980) 426.
- [7] W. Paik and Z. Szklarska-Smialowska, *Surface Sci.* 96 (1980) 401.
- [8] Z.I. Kudryavtseva, V.A. Openkin, N.A. Zhuchkova, E.I. Khrushcheva and N.A. Shumilova, *Elektrokhimiya* 11 (1975) 1392.
- [9] B. MacDougall and M. Cohen, *J. Electrochem. Soc.* 121 (1974) 1152.
- [10] B. MacDougall and M.J. Graham, *J. Electrochem. Soc.* 128 (1981) 2321.
- [11] M. Okuyama and S. Haruyama, *Corrosion Sci.* 14 (1974) 1.
- [12] M.A. Hopper and J.L. Ord, *J. Electrochem. Soc.* 120 (1973) 183.
- [13] R.S. Schrebler Guzman, J.R. Vilche and A.J. Arvia, *J. Appl. Electrochem.* 9 (1979) 183.
- [14] Yu.N. Chernykh and A.A. Yakovleva, *Elektrokhimiya* 6 (1970) 1595.
- [15] I.A. Cherepkova, V.V. Syssoeva, A.L. Rotinyan and N.N. Milyutin, *Elektrokhimiya* 12 (1976) 114.
- [16] Landolt Börnstein, 6. Auflage, Teil 8 (Springer, Berlin, 1962) p. 1–8.
- [17] Landolt Börnstein, 6. Auflage, Teil 8 (Springer, Berlin, 1962) p. 2–198.
- [18] T. Ohtsuka, K. Schroner and K.E. Heusler, *J. Electroanal. Chem.* 93 (1978) 171.
- [19] B. Rao, Mechanism of Passivation of Nickel, PhD Thesis, University of Pennsylvania (1966).
- [20] S. Roberts, *Phys. Rev.* 114 (1959) 104.
- [21] Z. Szklarska-Smialowska and H. Oranowska, *Corrosion Sci.* 16 (1976) 355.
- [22] Yu.N. Chernykh and A.A. Yakovleva, *Elektrokhimiya* 7 (1971) 510.
- [23] P.W.T. Lu and S. Srinivasan, *J. Electrochem. Soc.* 125 (1978) 1416.
- [24] American Institute of Physics Handbook, 2nd ed. (1963) p. 6–114.
- [25] Z.I. Kudryavtseva, N.A. Shumilova, V.A. Openkin, N.A. Zhuchkova and E.I. Krushcheva, *Elektrokhimiya* 13 (1977) 608.
- [26] F.L. McCrackin, *Natl. Bur. Std. (US) Tech. Note* 479 (1969).
- [27] G. Blondeau, M. Froment and A. Hugot-Le Goff, *Compt. Rend. (Paris)* C271 (1970) 795.
- [28] W. Visscher and A. Damjonovic, *Ext. Abstr. No. 138, 27th ISE Meeting* (1976).

- [29] Yu.N. Chernykh and A.A. Yakovleva, *Elektrokhimiya* 7 (1971) 513.
- [30] J.L. Ord, *Surface Sci.* 56 (1976) 413.
- [31] H. Bode, K. Dehmelt and J. Witte, *Electrochim. Acta* 11 (1966) 1079;
Z. Anorg. Allgem. Chem. 366 (1969) 1.
- [32] J.F. Wolf, L.S.R. Yeh and A. Damjanovic, *Electrochim. Acta* 26 (1981) 409.
- [33] G. Milazzo and S. Caroli, *Tables of Standard Potentials* (Wiley, 1978).
- [34] W. Visscher and E. Barendrecht, *J. Appl. Electrochem.* 10 (1980) 269.
- [35] W. Visscher and E. Barendrecht, *J. Electroanal. Chem.* 154 (1983) 69.